the University of Massachusetts Computing Center for computer time.

Registry No. $(C_6H_4O_2)_2PCl$, 6857-81-4.

Supplementary Material Available: A compilation of observed and calculated structure factor amplitudes (9 pages). Ordering information is given on any current masthead page.

References and Notes

(1) (a) Pentacoordinated Molecules. 25. Presented in part at the 173rd National Meeting of the American Chemical Society, New Orleans, La., March 1977; see Abstracts, No. INOR 168. (b) Previous paper in this series: J. A. Deiters, J. C. Gallucci, T. E. Clark, and R. R. Holmes, *J. Am. Chem. Soc.*, **99**, 5461 (1977).
(2) This work represents a portion of the Ph.D. Thesis of Richard K. Brown, University of Massachusetts, Amherst, Mass.
(3) (a) J. R. Devillers and R. R. Holmes, *J. Am. Chem. Soc.*, **99**, 3332 (1977); (b) J. S. Szobota and R. R. Holmes, *Inorg. Chem.*, following paper in this issue.
(4) (a) H. Wunderlich, D. Mootz, R. Schmutzler, and M. Wieber, *Z. Naturforsch. B*, **29**, 32 (1974); (b) H. Wunderlich, *Acta Crystallogr., Sect. B*, **30**, 939 (1974); (c) H. Wunderlich and D. Mootz, *ibid.*, **30**, 935 (1974).
(5) R. K. Brown and R. R. Holmes, *J. Am. Chem. Soc.*, 99, 3326 (1977).
(6) P. F. Meunier, J. A. Deiters, and R. R. Holmes, *Inorg. Chem.*, **15**, 2572 (1976).
(7) P. F. Meunier, J. R. Devillers, and R. R. Holmes, work submitted for publication.
(8) R. Sarma, F. Ramirez, and J. F. Maracek, *J. Org. Chem.*, **41**, 473 (1976).
(9) D. D. Swank, C. N. Caughlan, F. Ramirez, and J. F. Pilot, *J. Am. Chem. Soc.*, **93**, 5236 (1971).
(10) R. Sarma, F. Ramirez, B. McKeever, J. F. Maracek, and S. Lee, *J. Am. Chem. Soc.*, **98**, 581 (1976).
(11) R. D. Spratley, W. C. Hamilton, and J. Ladell, *J. Am. Chem. Soc.*, **89**, 2272 (1967).
(12) W. C. Hamilton, J. S. Ricci, Jr., F. Ramirez, L. Kramer, and P. Stern, *J. Am. Chem. Soc.*, **95**, 6335 (1973).
(13) D. Hellwinkel, W. Krapp, D. Schomburg, and W. S. Sheldrick, *Z. Naturforsch. B*, **31**, 948 (1976).
(14) (a) W. S. Sheldrick, A. Schmidpeter, and J. H. Weinmaier, *Angew. Chem.*, **87**, 519 (1975); (b) W. S. Sheldrick, *Acta Crystallogr., Sect. B*, **32**, 925 (1976).
(15) A. Schmidpeter, D. Schomburg, W. S. Sheldrick, and J. H. Weinmaier, *Angew. Chem.*, **88**, 85 (1976).
(16) W. S. Sheldrick, personal communication.
(17) M. Eisenhut, R. Schmutzler, and W. S. Sheldrick, *J. Chem. Soc., Chem. Commun.*, 144 (1973), and personal communication.
(18) H. A. E. Aly, J. H. Barlow, D. R. Russell, D. J. H. Smith, M. Swindles, and S. Trippett, *J. Chem. Soc., Chem. Commun.*, 449 (1976).
(19) J. A. Howard, D. R. Russell, and S. Trippett, *J. Chem. Soc., Chem. Commun.*, 856 (1973).
(20) (a) R. R. Holmes and J. A. Deiters, *J. Am. Chem. Soc.*, **99**, 3318 (1977); (b) R. R. Holmes and J. A. Deiters, *J. Chem. Res.*, No. 5, 92 (1977).
(21) R. S. Berry, *J. Chem. Phys.*, **32**, 933 (1960).
(22) (a) R. R. Holmes, *J. Am. Chem. Soc.*, **96**, 4143 (1974); (b) *ibid.*, **97**, 5379 (1975).
(23) R. R. Holmes, R. M. Deiters, and T. E. Clark, Abstracts, XVIIth International Conference on Coordination Chemistry, Hamburg, Germany, Sept 1976, p 21.
(24) (a) N. L. Allinger, M. A. Miller, F. A. Van Catledge, and J. A. Hirsch, *J. Am. Chem. Soc.*, **89**, 4345 (1967); (b) N. L. Allinger, M. T. Tribble, M. A. Miller, and D. H. Wertz, *ibid.*, **93**, 1637 (1971).
(25) J. A. Deiters, J. C. Gallucci, and R. R. Holmes, Abstracts, 173rd National Meeting of the American Chemical Society, New Orleans, La., March 1977, No. PHYS 269.
(26) R. R. Holmes, *Int. J. Peptide Protein Res.*, **8**, 445 (1976), and references cited therein.
(27) E. L. Muetterties, W. Mahler, and R. Schmutzler, *Inorg. Chem.*, **2**, 613 (1963).
(28) R. Hoffmann, J. M. Howell, and E. Muetterties, *J. Am. Chem. Soc.*, **94**, 3047 (1972).
(29) R. Lukenbach, "Dynamic Stereochemistry of Pentacoordinated Phosphorus and Related Elements", Georg Thieme Publishing Co., Stuttgart, 1973, and references cited therein.
(30) H. Oberhammer and J. Grobe, *Z. Naturforsch. B*, **30**, 506 (1975).
(31) F. Ramirez, A. J. Bigler, and C. P. Smith, *Tetrahedron*, **24**, 5049 (1968).
(32) Cell refinement and data collection were carried out using a package of rountines supplied by Enraf-Nonius Inc. for use with the PDP-8E computer.
(33) (a) G. Germain, P. Main, and M. M. Woolfson, *Acta Crystallogr., Sect. A*, **27**, 368 (1971); (b) T. Debaerdemaeker and M. M. Woolfson, *ibid.*, **28**, 477 (1972).
(34) Scattering factors used in SFLS-5 for nonhydrogen atoms were taken from D. T. Cromer and J. T. Waber, *Acta Crystallogr.*, **18**, 104 (1965); scattering factors for hydrogen atoms were taken from R. F. Stewart, E. R. Davidson, and W. T. Simpson, *J. Chem. Phys.*, **42**, 3175 (1965).
(35) D. W. J. Cruickshank in "Computing Methods in Crystallography", J. S. Rollett, Ed., Pergamon Press, Oxford, 1965, p 112.
(36) (a) W. R. Busing and H. A. Levy, *J. Chem. Phys.*, **26**, 563 (1957); (b) R. C. G. Killean, D. F. Grant, and J. L. Lawrence, *Acta Crystallogr., Sect. B*, **25**, 374 (1969).
(37) W. J. Adams and L. S. Bartell, *J. Mol. Struct.*, **8**, 23 (1971).
(38) (a) R. G. Cavell, D. D. Poulin, K. I. The, and A. J. Tomlinson, *J. Chem. Soc., Chem. Commun.*, 19 (1974); (b) D. D. Poulin and R. G. Cavell, *Inorg. Chem.*, **13**, 2324 (1974); (c) *ibid.*, **13**, 3012 (1974).
(39) (a) J. E. Griffiths, *J. Chem. Phys.*, **41**, 3510 (1964); (b) J. E. Griffiths and A. L. Beach, *ibid.*, **44**, 2686 (1966).
(40) K. W. Hansen and L. S. Bartell, *Inorg. Chem.*, **4**, 1775 (1965).
(41) R. R. Holmes, *Acc. Chem. Res.*, **5**, 296 (1972).

Contribution from the Department of Chemistry, University of Massachusetts, Amherst, Massachusetts 01003

Crystal and Molecular Structure of 2,2,3,3-Tetramethyl-5-dimethylamino-7,8-diphenyl-1,4,6,9-tetraoxa-5-phospha(P^V)spiro-[4.4]non-7-ene, $(C_6H_{12}O_2)(C_{14}H_{10}O_2)PN(CH_3)_2$[1]

JOHN S. SZOBOTA[2] and ROBERT R. HOLMES*

Received December 13, 1976 AIC60883C

The crystal structure of 2,2,3,3-tetramethyl-5-dimethylamino-7,8-diphenyl-1,4,6,9-tetraoxa-5-phospha(P^V)spiro[4.4]non-7-ene, $(C_6H_{12}O_2)(C_{14}H_{10}O_2)PN(CH_3)_2$ has been determined by single-crystal x-ray diffraction analysis. The compound crystallizes in the monoclinic space group $P2_1/c$ with cell constants a = 11.379 (3) Å, b = 12.646 (4) Å, c = 15.848 (4) Å, β = 102.25 (5)°, and Z = 4. Based on the dihedral angle method, the structural deviations from an idealized trigonal bipyramid (TP) indicate that this derivative is 31% along the Berry ligand exchange coordinate toward the idealized rectangular pyramid (RP). Pertinent features of the molecule are the O_{ax}–P–O_{ax} angle, 169.7 (1)°, the O_{eq}–P–O_{eq} angle, 129.9 (1)°, the near equality of P–O_{eq} and P–O_{ax} bond lengths of the saturated ring, 1.660 (1) and 1.662 (1) Å, respectively, with the P–O_{eq} bond length of the unsaturated ring, 1.673 (1) Å, and the planar configuration of the dimethylamino group which is rotated out of the equatorial plane by a torsional angle of 62°. The direction of rotation is such that repulsions between the *N*-methyl groups and the methyl group on the flap carbon atom of the saturated ring are minimized.

Introduction

From an estimation of ring strain in small-membered cyclic containing phosphoranes, the conclusion was reached that increasing ring unsaturation favors the appearance of a square or rectangular pyramid (SP, RP) compared to a trigonal bipyramid (TP).[3] Based on an electron pair repulsion argument, when the ring atoms directly bonded to phosphorus are of the same type, increasing atom electronegativity, as well, favors the SP(RP).[3,4]

We have carried out x-ray diffraction studies on the derivatives, I–V.[1b,5-7] These derivatives were chosen to test the generality of the above hypotheses. The present study concerns

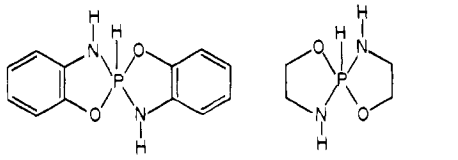

I[5] II[5,6]

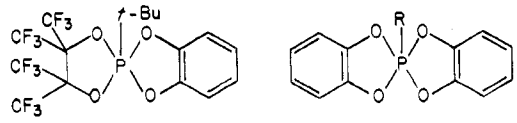

III[7a] IV,[1b] R = Cl; V,[7b] R = Ph

the single-crystal analysis of the dimethylaminophosphorane, VI. Inclusion of this member in the series allows the degree

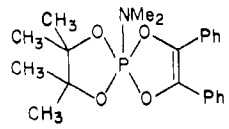

VI

of ring unsaturation to remain similar to that of III but provides a variation in the electronegativity term by substitution of methyl groups for perfluoro methyls.

Comparisons of structural details among members of this series I–VI and related derivatives suggests the main factors[8] which are important in structuring five-coordinate transition state analogues for reaction mechanism[9] of cyclic phosphates undergoing nucleophilic attack.

Experimental Section

Preparation of VI. Crystals of 2,2,3,3-tetramethyl-5-dimethylamino-7,8-diphenyl-1,4,6,9-tetraoxo-5-phospha(P^V)spiro[4.4]-7-nonene, $(C_6H_{12}O_2)(C_{14}H_{10}O_2)PN(CH_3)_2$, VI, were obtained by the addition of 2-dimethylaminotetramethyl-4,5-dioxaphospholane 1-3-2 to an equivalent of benzil in ether at room temperature according to the preparation of Bernard and Burgada.[10] Recrystallization from ether produced crystals suitable for x-ray structural analysis. The x-ray study was carried out on crystals enclosed in thin-walled glass capillaries because of the hygroscopic character of the compound (mp 156 °C, lit.[10] mp 156 °C).

Data Collection. Preliminary precession and Weissenberg photographs indicated the monoclinic system (Laue symmetry $2/m$). The absences $0k0$, $k = 2n + 1$, and $h0l$, $l = 2n + 1$, are consistent with the space group $P2_1/c$.

For data collection, a well-formed crystal of dimensions 0.30 × 0.35 × 0.45 mm was mounted on an Enraf-Nonius CAD-4 diffractometer with the crystal b axis nearly parallel with the instrument ϕ axis. Zr-filtered Mo radiation was used. The unit cell dimensions were obtained from least-squares refinement of the accurate setting angles of 15 high order reflections.[11] Of the total of 3633 independent reflections, 2411 were treated as observed (intensity greater than $0.1\sigma(I)$). The remaining 1222 reflections were assigned $F_o = [(1/Lp)(0.10\sigma(I)]^{1/2}$ where Lp is the standard Lorentz–polarization factor. Corrections for Lorentz and polarization effects were applied, but because of the small linear absorption coefficient ($\mu_{Mo} = 1.62$ cm^{-1}), no absorption corrections were made. A listing of experimental quantities associated with data collection is given in Table I.

Structure Determination and Refinement. Computations were carried out on a CDC 6600 computer (Model Cyber 74-18) using programming techniques and atom scattering factors, as cited.[1b,7b] Application of the direct methods program MULTAN resulted in eight sets of phases for the 350 reflections with the largest E values. The best-fit set was the only set that was chemically reasonable and yielded preliminary fractional coordinates for 22 of the 28 nonhydrogen atoms present.

Two cycles of isotropic full-matrix least-squares refinement (unit weight) and a subsequent electron density map were sufficient to locate the other six nonhydrogen atoms. Two further cycles of least-squares refinement led to the value of $R = 0.188$ for the 3633 independent reflections. Assignment of anisotropic thermal parameters and variable weight (given by $1/\sigma(F)^2$) resulted in values of $R = 0.122$ and $R_w = 0.105$ after five further cycles using 3633 reflections. A difference electron density map revealed the positions of the 28 independent hydrogen atoms.

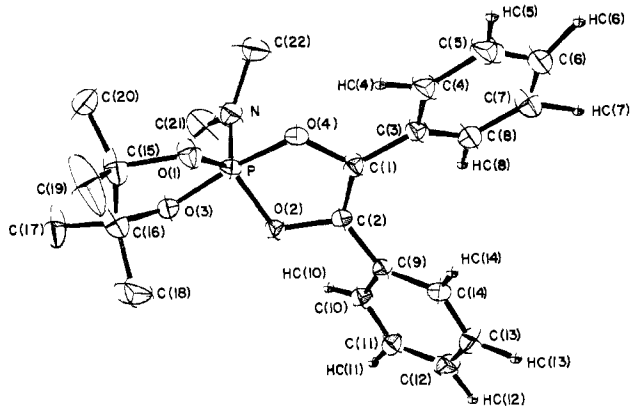

Figure 1. Molecular structure of $(C_6H_{12}O_2)(C_{14}H_{10}O_2)PN(CH_3)_2$ with thermal ellipsoids for nonhydrogen atoms shown at the 50% probability level. For purposes of clarity, hydrogen atoms are represented by spheres of arbitrary radius. (C. K. Johnson's ORTEP program, Report ORNL-3794, Oak Ridge National Laboratory, 1965.)

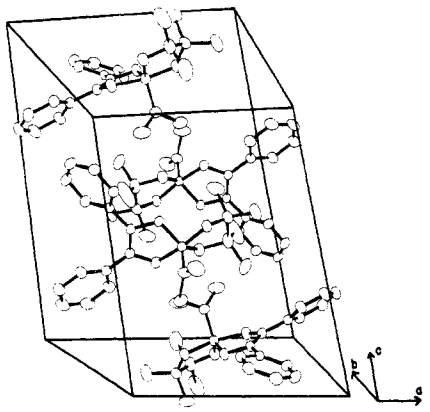

Figure 2. Unit cell ORTEP drawing of $(C_6H_{12}O_2)(C_{14}H_{10}O_2)PN(CH_3)_2$.

Further anisotropic refinement of the nonhydrogen atoms and isotropic refinement of the hydrogen atoms led to final values of $R = 0.041$ and $R_w = 0.028$ for the 2039 independent reflections having $F > 1.0\sigma(F)$. During the last cycle of refinement, the largest shift for any nonhydrogen atom parameter was $0.07\sigma_p$, and the largest shift for any hydrogen parameter was $0.19\sigma_p$, where σ_p is the standard error for the parameter in question.

The last cycles of refinement, repeated using all 3633 independent reflections, gave values of $R = 0.087$ and $R_w = 0.030$. No significant differences were observed between the parameters from this refinement and the final parameters obtained using the truncated data set. The maximum density on a final difference Fourier using 3633 reflections was 0.30 e/Å^3. A complete list of the final agreement indices is given in Table I. The positional and thermal parameters from the final cycle of least-squares refinement are presented in Tables II and III.

Results and Discussion

Bond lengths and angles for VI are listed in Tables IV and V, respectively. The molecular geometry is shown in Figure 1 and the packing arrangement in the unit cell is displayed in Figure 2. There are no short intermolecular contacts in the unit cell. Some intramolecular nonbonded distances are listed in Table VI.

The TP represents the general frame for the geometry of VI. However, the principal bond parameters given in Figure 3 show that there are significant structural distortions from

Table I. Experimental Details of the X-Ray Diffraction Study of $(C_6H_{12}O_2)(C_{14}H_{10}O_2)PN(CH_3)_2$

(A) Crystal Parameters at 23 ± 2 °C

Derived Standard Unit Cell Used in Refinement

a = 11.379 (3) Å
b = 12.646 (4) Å
c = 15.848 (4) Å
β = 102.25 (5)°
Space group: $P2_1/c$ [C_{2h}^5; No. 14]
Data for cell
Vol = 2122 (1) Å^3
Z = 4
Mol wt = 401.4
ρ(calcd) = 1.256 g cm^{-3}
ρ(obsd)[a] = 1.26 (2) g cm^{-3}

(B) Measurement of Intensity Data

Instrument:[b] Enraf-Nonius low-circle CAD-4 diffractometer controlled by a PDP8/e computer
Radiation: Mo K (Zr-filtered) $\lambda_{K\alpha_1}$ = 0.709 26 Å, $\lambda_{K\alpha_2}$ = 0.713 54 Å
Takeoff angle: 6.50 (5)°
Reflections measured: 3633 in the region $\pm h, +k, +l$ having $2° < 2\theta < 60°$
Crystal orientation: aligned approximately along [100]
Scan range: $\Delta(2\theta) = (0.8 + 0.5 \tan\theta)°$ centered about the average peak position
Scan type: θ-2θ
Standard reflections: intensity control ($6\bar{1}\bar{1}$); orientation control ($\bar{4}5\bar{3}$, $\bar{4}3\bar{7}$, 453) measured every 50 reflections; no significant deviation from average was observed

(C) Treatment of Intensity Data

Conversion to I and (I)

$I = [P - 2(B_1 + B_2)](1/n_s)^c$
(P = total count, B = background)
$\sigma(I) = [(P + 4(B_1 + B_2))(1/n_s^2) + (0.045I)^2]^{1/2}$
μ_{Mo} = 1.62 cm^{-1}

(D) Agreement Indices of Least-Squares Refinement

n (no. of variables) = 365
m/n (overdetermination ratio) = 5.6
$S = [\Sigma w(|F_o| - |F_c|)^2/(m-n)]^{1/2}$, 0.39
$R = [\Sigma||F_o| - |F_c||/\Sigma|F_o|]$, 0.041
$R_w = [\Sigma w(|F_o| - |F_c|)^2/\Sigma w(F_o)^2]^{1/2}$, 0.028

[a] Density as determined by the flotation method in a carbon tetrachloride–benzene mixture. [b] Experimental details of this instrument have been previously described.[7b] [c] The scan speed used for each reflection during data collection depended on the number of counts accumulated during a prescan and was given by $20.1166/n_s$. A factor of $1/n_s$ is therefore required to bring the intensities to the same scale.

Table II

(A) Atomic Coordinates for Nonhydrogen Atoms (×10^4) for $(C_6H_{12}O_2)(C_{14}H_{10}O_2)PN(CH_3)_2$ with Standard Deviations in Parentheses

Atom type[a]	x	y	z
P	4716.5 (5)	6711.8 (4)	6520.8 (4)
O(1)	4317 (1)	5458 (1)	6327 (1)
O(2)	5295 (1)	7573 (1)	5919 (1)
O(3)	3379 (1)	7153 (1)	6008 (1)
O(4)	6113 (1)	6166 (1)	6872 (1)
N	4644 (1)	7238 (1)	7463 (1)
C(1)	6990 (2)	6865 (2)	6727 (1)
C(2)	6551 (2)	7652 (2)	6162 (1)
C(3)	8214 (2)	6639 (2)	7208 (1)
C(4)	8539 (2)	5583 (2)	7480 (1)
C(5)	9676 (3)	5364 (3)	7957 (2)
C(6)	10502 (3)	6198 (3)	8154 (2)
C(7)	10191 (2)	7251 (3)	7901 (2)
C(8)	9051 (2)	7464 (2)	7434 (1)
C(9)	7074 (2)	8494 (2)	5697 (1)
C(10)	6472 (2)	9480 (2)	5478 (1)
C(11)	6912 (2)	10253 (2)	4985 (1)
C(12)	7953 (2)	10058 (2)	4705 (1)
C(13)	8561 (2)	9088 (2)	4923 (1)
C(14)	8136 (2)	8313 (2)	5415 (1)
C(15)	3039 (2)	5276 (2)	6017 (2)
C(16)	2620 (2)	6343 (2)	5536 (1)
C(17)	1321 (2)	6656 (3)	5487 (2)
C(18)	2914 (3)	6354 (4)	4617 (2)
C(19)	2892 (5)	4261 (4)	5465 (6)
C(20)	2505 (3)	5154 (4)	6827 (3)
C(21)	3870 (4)	8160 (3)	7560 (2)
C(22)	5229 (4)	6727 (4)	8275 (2)

(B) Refined Parameters for Hydrogen Atoms (×10^3) in $(C_6H_{12}O_2)(C_{14}H_{10}O_2)PN(CH_3)_2$ with Standard Deviations in Parentheses

Atom type[a]	x	y	z	B_{iso}, Å^2
HC4	794 (2)	500 (1)	736 (1)	5 (1)
HC5	988 (2)	461 (2)	811 (1)	6 (1)
HC6	1121 (2)	600 (2)	845 (1)	7 (1)
HC7	1077 (2)	791 (2)	804 (1)	9 (1)
HC8	885 (1)	821 (1)	726 (1)	5 (1)
HC10	574 (1)	963 (1)	571 (1)	4 (1)
HC11	644 (2)	1095 (1)	485 (1)	6 (1)
HC12	825 (2)	1062 (1)	434 (1)	6 (1)
HC13	927 (1)	895 (1)	471 (1)	4 (1)
HC14	856 (1)	761 (1)	557 (1)	4 (1)
HC17(1)	83 (2)	607 (2)	517 (1)	8 (1)
HC17(2)	136 (2)	678 (2)	625 (1)	8 (1)
HC17(3)	113 (2)	723 (2)	512 (1)	8 (1)
HC18(1)	263 (3)	698 (3)	436 (2)	15 (2)
HC18(2)	225 (3)	578 (2)	428 (2)	14 (1)
HC18(3)	386 (3)	576 (3)	469 (2)	19 (1)
HC19(1)	207 (2)	421 (2)	523 (1)	7 (1)
HC19(2)	347 (3)	427 (3)	515 (3)	16 (2)
HC19(3)	304 (3)	372 (3)	595 (2)	12 (1)
HC20(1)	163 (2)	488 (2)	663 (2)	13 (1)
HC20(2)	291 (2)	454 (2)	712 (2)	12 (1)
HC20(3)	250 (3)	597 (3)	711 (2)	21 (2)
HC21(1)	314 (2)	784 (2)	764 (2)	12 (1)
HC21(2)	428 (2)	860 (2)	814 (2)	13 (1)
HC21(3)	375 (2)	856 (2)	706 (2)	10 (1)
HC22(1)	488 (3)	695 (2)	868 (2)	12 (1)
HC22(2)	597 (3)	723 (4)	844 (3)	23 (2)
HC22(3)	542 (2)	602 (2)	817 (2)	11 (1)

[a] Atoms are named to agree with Figure 1. Hydrogen atoms are named according to the carbon atoms to which they are bonded.

the idealized form. The equatorial angles at phosphorus, O(1)–P–O(2) and O(2)–P–N, are respectively opened and closed by about 10° relative to the 120° value in the TP. There is a concomitant decrease in the axial O(3)–P–O(4) angle to 169.7 (1)° from the 180° value in the ideal TP. The direction of displacement of the four oxygen atoms is consistent with the angle bending which takes place in the Berry ligand exchange process.[12] Movement along this distortion coordinate from the idealized TP toward the RP representation with the nitrogen acting as the pivotal ligand is suggested from these data.

Quantitative evaluation of the degree of displacement along the Berry coordinate by the dihedral angle method, which we have previously applied,[8] places VI 30.7% from the TP toward the idealized RP. The dihedral angles calculated from polyhedral surfaces defined by the positions of the five atoms attached to phosphorus are listed in Table VII.

As seen from the dihedral angle sums in footnote *c* of Table VII, the structure is directly on the Berry coordinate. In accord, the least-squares planes I (axial) and IV (equatorial) of Table VIII show small atom displacements and make a dihedral angle with each other of 86.5°. The latter angle is in the range expected, 90–85.9°, if a local C_{2v} constraint is followed for angle variations along the Berry coordinate leading to the idealized RP.

With regard to bond distance variations, which normally are longer for axial bonds containing like ligands compared

Table III. Thermal Parameters for Nonhydrogen Atoms for $(C_6H_{12}O_2)(C_{14}H_{10}O_2)PN(CH_3)_2$ with Standard Deviations in Parentheses

Atom type[a]	Anisotropic parameters[b]						Equivalent[c] isotropic B
	B_{11}	B_{22}	B_{33}	B_{12}	B_{13}	B_{23}	
P	3.08 (2)	3.49 (3)	3.65 (3)	−0.05 (2)	0.42 (2)	0.71 (3)	3.38
O(1)	3.8 (1)	3.6 (1)	5.9 (1)	−0.2 (1)	0.2 (1)	−0.1 (1)	4.4
O(2)	2.8 (1)	4.3 (1)	4.3 (1)	0.0 (1)	0.4 (1)	1.4 (1)	3.6
O(3)	3.0 (1)	4.1 (1)	5.2 (1)	−0.2 (1)	0.0 (1)	0.8 (1)	4.0
O(4)	3.1 (1)	4.5 (1)	5.3 (1)	−0.1 (1)	0.3 (1)	1.7 (1)	4.1
N	4.8 (1)	5.3 (1)	3.7 (1)	0.5 (1)	0.4 (1)	−0.1 (1)	4.6
C(1)	3.1 (1)	3.4 (1)	3.9 (1)	0.0 (1)	0.3 (1)	0.4 (1)	3.5
C(2)	2.5 (1)	3.8 (1)	3.9 (1)	−0.2 (1)	0.3 (1)	0.7 (1)	3.4
C(3)	3.3 (1)	4.0 (1)	3.6 (1)	0.5 (1)	0.4 (1)	0.2 (1)	3.6
C(4)	4.4 (1)	5.2 (2)	4.5 (1)	1.1 (1)	0.4 (1)	0.1 (1)	4.7
C(5)	5.5 (2)	7.2 (2)	5.4 (2)	2.9 (2)	0.7 (1)	1.0 (1)	5.6
C(6)	3.5 (2)	12.9 (3)	4.7 (2)	2.2 (2)	−0.4 (1)	0.8 (1)	5.8
C(7)	4.2 (2)	9.8 (2)	5.2 (1)	−0.5 (2)	−0.4 (1)	0.6 (2)	6.0
C(8)	3.8 (1)	5.6 (2)	4.9 (1)	−0.1 (1)	−0.2 (1)	0.5 (1)	4.8
C(9)	2.7 (1)	3.6 (1)	3.2 (1)	−0.1 (1)	0.1 (1)	0.2 (1)	3.2
C(10)	3.3 (1)	4.6 (1)	4.1 (1)	0.0 (1)	0.5 (1)	0.8 (1)	3.9
C(11)	4.5 (1)	4.3 (1)	4.8 (1)	−0.5 (1)	−0.1 (1)	1.1 (1)	4.5
C(12)	5.0 (1)	5.6 (2)	4.6 (1)	−1.8 (1)	0.6 (1)	1.1 (1)	4.8
C(13)	4.2 (1)	6.4 (2)	4.9 (1)	−0.8 (1)	1.8 (1)	0.1 (1)	4.8
C(14)	3.7 (1)	4.3 (1)	4.2 (1)	−0.1 (1)	0.9 (1)	0.2 (1)	4.1
C(15)	3.8 (1)	4.2 (1)	7.9 (2)	−0.7 (1)	0.2 (1)	−0.6 (1)	5.0
C(16)	3.8 (1)	5.7 (2)	4.7 (1)	0.0 (1)	−0.3 (1)	−0.5 (1)	4.8
C(17)	3.7 (1)	6.8 (2)	10.6 (2)	−0.8 (1)	−0.9 (1)	0.1 (2)	6.5
C(18)	9.1 (2)	13.9 (3)	4.0 (2)	1.0 (2)	0.1 (1)	−1.0 (2)	8.0
C(19)	8.1 (3)	7.0 (3)	20.5 (5)	0.3 (3)	−5.4 (3)	−6.2 (3)	8.9
C(20)	5.7 (2)	11.0 (3)	11.5 (3)	−1.4 (2)	2.7 (2)	5.1 (3)	7.7
C(21)	8.1 (2)	8.0 (2)	6.3 (2)	1.7 (2)	0.5 (2)	−2.7 (2)	7.0
C(22)	11.2 (3)	7.8 (2)	4.1 (2)	1.3 (2)	0.8 (2)	0.5 (2)	7.1

[a] Atoms named to agree with Figure 1. [b] Anisotropic thermal parameters used during refinement were of the form $\exp[-(\beta_{11}h^2 + \beta_{22}k^2 + \beta_{33}l^2 + 2\beta_{12}hk + 2\beta_{13}hl + 2\beta_{23}kl)]$. The B_{ij}'s in Å^2 are derived from the dimensionless β_{ij}'s by $B_{ij} = 4\beta_{ij}/a_i^* a_j^*$. [c] Equivalent isotropic B's $= 4[V^2 \det(\beta_{ij})]^{1/3}$.

Table IV. Bond Distances (Å) and Standard Deviations (in Parentheses) for $(C_6H_{12}O_2)(C_{14}H_{10}O_2)PN(CH_3)_2$

Bond	Distance	Bond	Distance
P-O(1)	1.660 (1)	N-C(22)	1.468 (4)
P-O(2)	1.673 (1)	C(4)-HC4	0.99 (2)
P-O(3)	1.662 (1)	C(5)-HC5	0.99 (2)
P-O(4)	1.713 (1)	C(6)-HC6	0.88 (2)
P-N	1.652 (2)	C(7)-HC7	1.06 (2)
O(1)-C(15)	1.452 (2)	C(8)-HC8	0.99 (1)
O(2)-C(2)	1.402 (2)	C(10)-HC10	1.00 (2)
O(3)-C(16)	1.443 (2)	C(11)-HC11	1.03 (2)
O(4)-C(1)	1.388 (2)	C(12)-HC12	1.01 (2)
C(1)-C(2)	1.361 (3)	C(13)-HC13	0.96 (2)
C(1)-C(3)	1.466 (3)	C(14)-HC14	1.01 (2)
C(3)-C(4)	1.427 (3)	C(17)-HC17(1)	1.00 (2)
C(4)-C(5)	1.381 (4)	C(17)-HC17(2)	1.22 (2)
C(5)-C(6)	1.403 (5)	C(17)-HC17(3)	0.92 (2)
C(6)-C(7)	1.414 (6)	C(18)-HC18(1)	0.91 (3)
C(7)-C(8)	1.377 (3)	C(18)-HC18(2)	1.10 (3)
C(8)-C(3)	1.407 (3)	C(18)-HC18(3)	1.30 (3)
C(2)-C(9)	1.490 (3)	C(19)-HC19(1)	0.94 (2)
C(9)-C(10)	1.430 (3)	C(19)-HC19(2)	0.90 (4)
C(10)-C(11)	1.407 (3)	C(19)-HC19(3)	1.02 (3)
C(11)-C(12)	1.374 (3)	C(20)-HC20(1)	1.03 (3)
C(12)-C(13)	1.415 (4)	C(20)-HC20(2)	0.97 (3)
C(13)-C(14)	1.400 (3)	C(20)-HC20(3)	1.13 (4)
C(14)-C(9)	1.393 (3)	C(21)-HC21(1)	0.95 (3)
C(15)-C(19)	1.542 (7)	C(21)-HC21(2)	1.09 (3)
C(15)-C(20)	1.540 (5)	C(21)-HC21(3)	0.92 (3)
C(15)-C(16)	1.573 (3)	C(22)-HC22(1)	0.87 (3)
C(16)-C(17)	1.516 (3)	C(22)-HC22(2)	1.04 (4)
C(16)-C(18)	1.562 (4)	C(22)-HC22(3)	0.95 (3)
N-C(21)	1.488 (4)		

Table V. Bond Angles (deg) and Standard Deviations (in Parentheses) for $(C_6H_{12}O_2)(C_{14}H_{10}O_2)PN(CH_3)_2$

Atoms	Angle	Atoms	Angle
O(3)-P-O(4)	169.68 (7)	O(3)-C(16)-C(18)	104.7 (2)
O(3)-P-O(2)	86.17 (6)	O(3)-C(16)-C(15)	105.7 (2)
O(3)-P-O(1)	92.50 (7)	C(15)-C(16)-C(17)	116.1 (2)
O(3)-P-N	95.17 (8)	C(15)-C(16)-C(18)	110.9 (2)
O(4)-P-O(2)	89.84 (6)	C(17)-C(16)-C(18)	110.5 (2)
O(4)-P-O(1)	82.77 (6)	O(2)-C(2)-C(9)	113.9 (2)
O(4)-P-N	95.14 (8)	O(2)-C(2)-C(1)	109.9 (2)
O(1)-P-O(2)	129.93 (7)	O(4)-C(1)-C(3)	115.2 (2)
O(2)-P-N	110.75 (8)	O(4)-C(1)-C(2)	113.4 (2)
O(1)-P-N	119.19 (8)	C(1)-C(2)-C(9)	136.0 (2)
P-N-C(21)	123.6 (2)	C(2)-C(1)-C(3)	131.3 (2)
P-N-C(22)	121.0 (2)	C(2)-C(9)-C(10)	121.5 (2)
C(21)-N-C(22)	114.9 (2)	C(2)-C(9)-C(14)	120.4 (2)
P-O(1)-C(15)	115.5 (1)	C(10)-C(9)-C(14)	118.0 (2)
P-O(3)-C(16)	113.6 (1)	C(9)-C(10)-C(11)	122.1 (2)
P-O(2)-C(2)	113.0 (1)	C(10)-C(11)-C(12)	119.2 (2)
P-O(4)-C(1)	109.9 (1)	C(11)-C(12)-C(13)	119.1 (2)
O(1)-C(15)-C(20)	106.2 (2)	C(12)-C(13)-C(14)	122.3 (2)
O(1)-C(15)-C(19)	107.7 (3)	C(13)-C(14)-C(9)	119.3 (2)
O(1)-C(15)-C(16)	101.9 (2)	C(1)-C(3)-C(8)	120.3 (2)
C(16)-C(15)-C(19)	117.0 (3)	C(1)-C(3)-C(4)	119.7 (2)
C(16)-C(15)-C(20)	111.0 (2)	C(8)-C(3)-C(4)	119.9 (2)
C(19)-C(15)-C(20)	112.0 (4)	C(3)-C(4)-C(5)	120.3 (2)
O(3)-C(16)-C(17)	108.1 (2)	C(4)-C(5)-C(6)	118.5 (3)
		C(5)-C(6)-C(7)	122.0 (3)
		C(6)-C(7)-C(8)	119.1 (2)
		C(7)-C(8)-C(3)	120.2 (2)

to equatorial bonds,[13] the present phosphorane shows an axial P–O(3) distance of 1.662 (1) Å, almost the same as the equatorial P–O(1) distance, 1.660 (1) Å, present in the saturated five-membered ring. Although data are limited for saturated five-membered rings, an equatorial P–O distance closer to 1.60 Å is expected.[8] For unsaturated five-membered rings, more data are available. From a recent tabulation,[8] for the percent of the Berry coordinate traversed for VI, the P–O distances should approximate 1.74 Å for an axial bond and 1.64 Å for an equatorial bond. The observed values are 1.713 (1) and 1.673 (1) Å, respectively, for the unsaturated ring. Again the P–O_{eq} bond appears somewhat elongated.

This may be partially a result of the presence of the planar dimethylamino group coupled with ring constraints and

Table VI. Some Intramolecular Nonbonded Distances (Å)

O(1)-O(2)	3.020 (2)	O(4)-C(22)	2.723 (4)
O(1)-O(3)	2.399 (2)	O(3)-HC21(3)	2.42 (3)
O(1)-O(4)	2.230 (2)	O(4)-HC22(3)	2.36 (3)
O(1)-N	2.857 (2)	C(21)-C(20)	4.177 (6)
O(2)-O(4)	2.391 (2)	C(21)-C(17)	4.334 (5)
O(2)-O(3)	2.278 (2)	C(22)-C(20)	3.977 (6)
O(2)-N	2.736 (2)	C(22)-C(17)	5.565 (5)
O(3)-O(4)	3.361 (2)	C(22)-O(3)	3.797 (4)
O(3)-N	2.447 (2)	C(21)-O(4)	3.903 (4)
O(4)-N	2.484 (2)	C(21)-O(3)	2.719 (4)

Table VII. Dihedral Angles (δ) for $(C_6H_{12}O_2)(C_{14}H_{10}O_2)PN(CH_3)_2$, VI, deg[a]

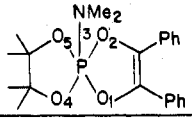

Edge[b]	δ[c]	Edge	δ
45	107.3	13	93.1
25	105.6	23	62.8
14	110.3	34	57.3
12	103.5	24	36.5
35	94.2		

[a] For purposes of comparison with a similar tabulation of dihedral angles for other compounds, the atom numbering scheme shown above is used where the subscripts 1 and 5 refer to axial type atoms, 2 and 4 refer to equatorial type atoms, and 3 refers to the equatorial pivotal atom in the Berry process. [b] The number pairs refer to the common edge connecting the two triangular faces whose normals give the dihedral angle. [c] The sum $\Sigma_i|\delta_i(C) - \delta_i(TP)| = 66.9°$ and the sum $\Sigma_i|\delta_i(C) - \delta_i(RP)| = 150.8°$. These two sums add up to 217.7° showing close correspondence with the Berry coordinate since $\Sigma_i|\delta_i(TP) - \delta_i(RP)| = 217.9°$. Refer to Table VIII of ref 1b for the values of the dihedral angles for the idealized TP and RP.

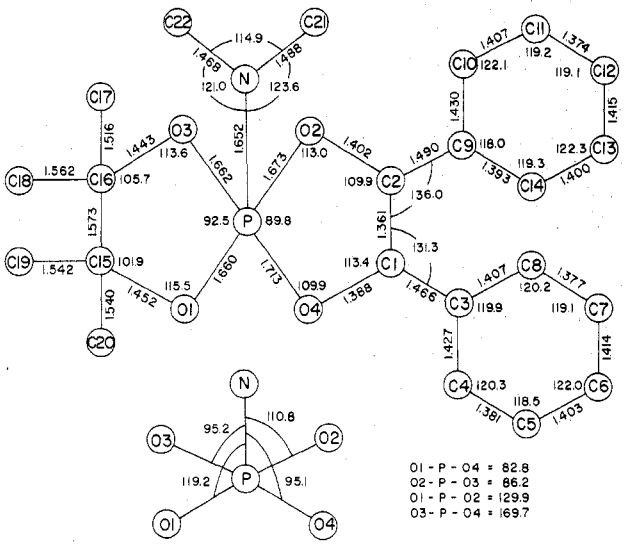

Figure 3. Schematic diagram of $(C_6H_{12}O_2)(C_{14}H_{10}O_2)PN(CH_3)_2$ showing principal bond parameters (distances, Å; angles, deg).

partially a result of nonbonded repulsions between the amino methyl groups and the axial oxygen atoms. As electron pair repulsion from the P–N bond (due to back-donation of the lone pair on nitrogen in p–d π bonding) reinforced by nonbonded repulsions from the $N(CH_3)_2$ group causes the nearer axial P–O bonds to bend away, ring constraints, which are more severe in the unsaturated ring,[3] are best relieved by a lengthening of the equatorial bonds. In the absence of ring constraints, in CH_3PF_4[14] for example, the lengthening of all P–F bonds, and angle bending away from the equatorial P–CH_3 bond, is accountable[15] by the increased electron pair

Table VIII. Atom Distances from Mass Weighted Least-Squares Planes (Å)[a]

	Plane[b] I	II	III	IV	V
P	−0.019	0.023	−0.001	0.002	−0.009
O(1)	0.013				0.036
O(2)	0.009	−0.112			
O(3)				−0.003	0.059
O(4)		−0.125		−0.003	
N	0.018		−0.043	0.001	
C(1)		0.146			
C(2)		0.111			
C(15)					(0.403)
C(16)					−0.104
C(21)			0.027		
C(22)			0.026		

	Plane[b] VI	VII		VIII	
C(3)	−0.006	C(9)	−0.004	O(2)	0.004
C(4)	0.002	C(10)	0.002	O(4)	−0.005
C(5)	0.009	C(11)	0.002	C(1)	0.022
C(6)	−0.012	C(12)	−0.004	C(2)	−0.021
C(7)	−0.0001	C(13)	−0.0005	P	(0.365)
C(8)	0.007	C(14)	0.004		
C(1)	(0.032)	C(2)	(−0.105)		

[a] Distances enclosed by parentheses denote distances from least-squares plane of atoms not included in least-squares plane calculation. [b] Some dihedral angles between least-squares planes are III and IV = 27.7°, II and V = 48.0°, I and IV = 86.5°, and VI and VII = 53.7°.

repulsion effects due to the presence of the P–C bond compared to that in PF_5. The pronounced axial bending observed in VI contributes then to the widening of the equatorial angle, O(1)–P–O(2), to 129.9 (1)° in order to minimize nonbonded repulsions among the oxygen atoms. We suspect that the reason the O(1)–P–N equatorial angle is larger than the O(2)–P–N equatorial angle is associated with the direction of rotation of the $(CH_3)_2N$ group and the attainment of a configuration of minimum repulsion with respect to the methyls attached to the flap atom, C_{15} (as discussed later).

The related cyclic phosphorane, VII, containing a planar

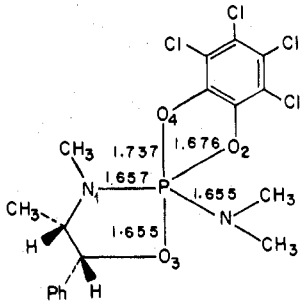

(distances, Å)

VII

dimethylamino group and the presence of both a saturated and unsaturated five-membered ring, shows very similar P–O bond distances[16] to those in VI; although, the P–O axial distance in the unsaturated ring is now close to that predicted. The structure of VII[16] is distorted in a manner very similar to that in VI. The O_3–P–O_4 axial angle (171.3°) and the N_1–P–O_2 equatorial angle (125.2°) compare with 169.7 and 129.9°, respectively, for these angles in VI.

In each of these compounds, the plane of the dimethylamino group does not coincide with the axial plane. In the present study, a dihedral angle of 27.6° is obtained between the least-squares planes III and IV (Table VIII) showing that the $(CH_3)_2N$ group is rotated this amount relative to the axial plane (or, relative to the equatorial plane, a torsional angle

of 62° results). In the related phosphorane, VII, the magnitude of this torsional angle is the same. An electron diffraction study of tris(dimethylamino)difluorophosphorane,[17] VIII,

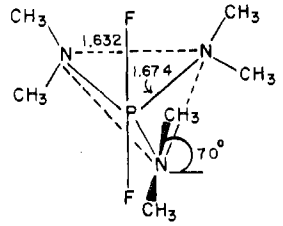

VIII[17]

yields a value of 70° for this angle. Theoretical calculations on NH_2PF_4 suggest that as the amino moiety rotates out of the most favored axial orientation, increasing pyramidal character is expected.[18] The above results on the dimethylamino derivatives, VI–VIII, give no evidence to support this contention.

In the latter acyclic derivative, the P–N bonds are longer than those in VI and VII and the P–F axial bonds of 1.632 (6) Å compare with 1.577 (5) Å for the P–F_{ax} bond length in PF_5.[19] Again, back-donation from nitrogen, resulting in cooperative electron pair repulsions, rationalizes the observed bond length data.

The direction of rotation of the dimethylamino group in VI results from minimum repulsion effects with the methyl group attached to the ring carbon atoms, C_{15} and C_{16}. Carbon atom C_{15} is the flap atom directed out of the least-squares plane V of Table VIII 0.4 Å toward the $(CH_3)_2N$ group. The torsional angle in the system O(1)–C(15)–C(16)–O(3) is 32.8°. This brings the methyl carbon C_{20} closest to C_{21} and C_{22} of the $(CH_3)_2N$ group and produces the counterclockwise P–N bond rotation (relative to the axial direction) indicated in Figure 1. If C_{16} were the flap atom, directed toward the $(CH_3)_2N$ group, calculation indicates that the attached methyl carbon C_{17} would be even closer to C_{21} and result in a greater repulsion effect.

The alternation in bond distances and bond angles in the unsaturated five-membered ring of VI is similar to that observed in other cyclic phosphoranes.[1b,7b] The occurrence is particularly pronounced as structures approach the TP and is attributable to ring strain minimization as a result of bond electron density variations.[3]

One further feature is worth noting, the disposition of the phenyl groups attached to the ethylenic bond. The relative canting of the phenyl rings is indicated by the dihedral angle of 53.7° between the least-squares planes VI and VII of Table VIII. Mutual repulsion of the phenyl groups, no doubt, contributes to some extent in accounting for the large exocyclic angles C(2)–C(1)–C(3) = 131.3 (2)° and C(1)–C(2)–C(9) = 136.0 (2)°. In a related bicyclic phosphorane, IX, the

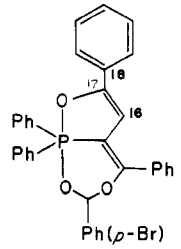

IX

C(18)–C(17)–C(16) angle is reported[20] as 129.0 (4)°. There is also a degree of nonplanarity in the ethylenic system in VI. The plane of the C(9)–C(2)–O(2) atoms makes an angle of 6.9° with the plane of the C(3)–C(1)–O(4) atoms. The planarity of the unsaturated ring is indicated by the least-squares plane VIII (Table VIII). The phosphorus atom is puckered 0.37 Å out of this plane on the side toward the $(CH_3)_2N$ group.

The percent displacement along the Berry coordinate from the TP to the RP for the cyclic phosphorane structures we have investigated[1b,5–7] is I (~23), II (28), III (38), IV (72), and V (72%). In the present study, we calculated 31% displacement for VI. Its position, showing greater displacement from the TP than I or II,[21] is consistent with the presence of four electronegative heterooxygen atoms directly attached to phosphorus.[3,4] The introduction of less electronegative methyl substituents on the saturated ring in place of perfluoromethyl groups appears to be a primary factor in causing VI to shift more toward the TP end of the distortion coordinate relative to III. For VII, we calculate 19.0%, showing the effect of the introduction of a heteroring nitrogen atom in reducing the displacement from the TP compared to that for VI.

In the related benzo derivative X, which contains two atoms

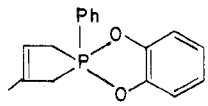

X

of low electronegativity in one unsaturated ring and two atoms of high electronegativity in the second unsaturated ring (directly bonded to phosphorus), the x-ray structure[22] shows it displaced near 93% toward the RP; i.e., of the examples so far encountered, its structure appears closest to a RP. This is a consequence of the poor axiophilicity for a carbon atom, so situated if a TP did form, and the relief of ring strain expected for a RP compared to that for a TP.[3] In the TP, an unsaturated five-membered ring with its associated rigidity encounters more strain when the ring heteroatoms are the same. In the idealized RP, the P–O bonds assume equal character.

Acknowledgment. The support for this research by the National Science Foundation (MPS 74-11496) and the National Institutes of Health (GM 21466) and the inclusion of funds by NSF for the purchase of an Enraf-Nonius CAD-4 diffractometer are gratefully acknowledged. We wish to thank Professor Roberta O. Day for her assistance in the structure refinement and the University of Massachusetts Computing Center for generous allocation of computer time.

Registry No. VI, 62930-62-5.

Supplementary Material Available: A compliation of observed and calculated structure factor amplitudes (23 pages). Ordering information is given on any current masthead page.

References and Notes

(1) (a) Pentacoordinated Molecules. 26. Presented in part at the 173rd National Meeting of the American Chemical Society, New Orleans, La., March 1977; see Abstracts, No. INOR 168. (b) Part 25: R. K. Brown and R. R. Holmes, *Inorg. Chem.*, preceding paper in this issue.
(2) (a) This work represents a portion of the Ph.D. Thesis of J. S. Szobota, University of Massachusetts, Amherst, Mass.
(3) R. R. Holmes, *J. Am. Chem. Soc.*, **97**, 5379 (1975).
(4) R. R. Holmes, *J. Am. Chem. Soc.*, **96**, 4143 (1974).
(5) P. F. Meunier, J. A. Deiters, and R. R. Holmes, *Inorg. Chem.*, **15**, 2572 (1976).
(6) P. F. Meunier, J. R. Devillers, R. O. Day, and R. R. Holmes, work submitted for publication.
(7) (a) R. K. Brown and R. R. Holmes, unpublished work; (b) *J. Am. Chem. Soc.*, **99**, 3326 (1977).
(8) R. R. Holmes and J. A. Deiters, *J. Am. Chem. Soc.*, **99**, 3318 (1977).
(9) R. Lukenbach, "Dynamic Stereochemistry of Pentacoordinated Phosphorus and Related Elements", Georg Thieme Publishing Co., Stuttgart, 1973, and references cited therein.
(10) D. Bernard and R. Burgada, *Tetrahedron*, **31**, 797 (1975).
(11) Cell refinement and data collection were carried out using a package of routines supplied by Enraf-Nonius, Inc., for use with the PDP8/e computer.
(12) R. S. Berry, *J. Chem. Phys.*, **32**, 933 (1960).

(13) R. R. Holmes, *Acc. Chem. Res.*, **5**, 296 (1972).
(14) L. S. Bartell and K. W. Hansen, *Inorg. Chem.*, **4**, 1777 (1965).
(15) R. J. Gillespie, *Inorg. Chem.*, **5**, 1634 (1966).
(16) R. Wolf and R. Weiss, personal communication.
(17) H. Oberhammer and R. Schmutzler, *J. Chem. Soc., Dalton Trans.*, 1454 (1976).
(18) A. Strich and A. Veillard, *J. Am. Chem. Soc.*, **95**, 5574 (1973).
(19) K. W. Hansen and L. S. Bartell, *Inorg. Chem.*, **4**, 1775 (1965).
(20) D. D. Swank, C. N. Caughlan, F. Ramirez, and J. F. Pilot, *J. Am. Chem. Soc.*, **93**, 5236 (1971).
(21) Derivative II which has saturated rings should have more TP character than I if the arguments referred to[3] here apply. The percent displacement[8] shows the opposite, however. As discussed in ref 5 and 6, intermolecular hydrogen bonding in II is responsible for the reversal. The molecules are so positioned in the unit cell that N—H···O hydrogen bonding acts to open the N_{eq}–P–N_{eq} angle. Although hydrogen bonding is present in I, the positioning of the neighboring oxygen atoms does not induce an appreciable effect of this type. Computer minimization via molecular mechanics bears this out.[5]
(22) J. R. Devillers and R. R. Holmes, *J. Am. Chem. Soc.*, **99**, 3332 (1977).

Contribution from the Fachbereich Naturwissenschaften II, Gesamthochschule, 5600 Wuppertal, West Germany

Crystal and Molecular Structure, Reinvestigated Vibrational Spectra, and Normal-Coordinate Analysis of Potassium (Trifluoromethyl)trifluoroborate, $K[CF_3BF_3]$[1]

D. J. BRAUER, H. BÜRGER,* and G. PAWELKE

Received January 12, 1977 AIC70015V

The structure and vibrational spectra of $K[CF_3BF_3]$ have been determined by x-ray diffraction methods and have been reinvestigated by IR and Raman spectroscopy, respectively. The compound crystallizes in the monoclinic space group C_{2h}^5-$P2_1/c$ with a = 4.843 (1) Å, b = 16.331 (4) Å, c = 6.348 (2) Å, β = 101.89 (3)°, Z = 4, d_c = 2.378 g cm^{-3}, and d_o = 2.5 (1) g cm^{-3}. The structure was refined anisotropically to a conventional R factor of 0.058 based on 767 counter measured, absorption corrected reflections with $|F_o| > 4\sigma(|F_o|)$. The compound forms ionic crystals which impose no crystallographic symmetry on the ions. The anion deviates somewhat from C_{3v} symmetry, the CF_3 and BF_3 groups being rotated about 8° from the staggered conformation. The average C–F, B–F, and B–C bond distances are 1.343 (8) Å (corrected 1.360 Å), 1.391 (5) Å (corrected 1.409 Å), and 1.625 (6) Å (corrected 1.640 Å), respectively, the values being corrected for libration. The F–C–F angle is 104.9 (2)°. IR spectra of KBr and polyethylene pellets in the 50–2000-cm^{-1} region and Raman spectra of aqueous solution, crystal powder, and single crystals were recorded on specimens with various ^{10}B:^{11}B ratios and assigned for a staggered C_{3v} model. A normal-coordinate analysis yielded a general harmonic valence force field which reproduces both frequencies and observed isotope shifts and which is consistent with that of related species. The following stretching force constants were obtained: f_{CF} = 4.85, f_{BF} = 4.19, and f_{BC} = 3.63 mdyn/Å. Bonding in CF_3B compounds is discussed on the basis of the x-ray and the spectroscopic data.

Introduction

In preceding papers[3] we have reported the vibrational spectra of CF_3 derivatives of group 4–7 elements and have demonstrated the efficiency of a normal-coordinate analysis for interpretation of spectra and description of vibrational properties. The only group 3 CF_3 derivatives which are reported to be stable at room temperature are CF_3BF_2[4] and the anion $CF_3BF_3^-$.[5,6] In addition to some other physical properties, unassigned IR spectra of CF_3BF_2[4] and salts of the $CF_3BF_3^-$ anion[5,6] have been reported. Recently[7] $K[CF_3BF_3]$ has been thoroughly investigated by means of IR and Raman spectroscopy. We disagree with results of this investigation for three reasons. (i) The quality of the Raman spectra obtained from crystalline powder and from aqueous solutions is not acceptable; the spectra cover only the $\Delta\nu$ < 1300-cm^{-1} region. With one exception no depolarization ratios have been obtained. Due to the use of a wide spectral slit, some individual lines could not be resolved and no $^{10/11}B$ isotope shifts could be determined precisely. (ii) The vibration predominantly involving the δ_s CF_3 (umbrella) motion is always connected with an intense Ra line at 750 ± 50 cm^{-1}; this feature should show only a very small $^{10/11}B$ shift in $CF_3BF_3^-$. The strongest Ra line of $CF_3BF_3^-$ indeed occurs at ~730 cm^{-1} and shows no shift. This line has been assigned, however, to ν_s BF_3 by Jackovitz et al.[7] while a band at ~970 cm^{-1} with a $^{10/11}B$ shift of 22 cm^{-1} has been attributed to a mode that is mainly ν_s CF_3 in character. Furthermore, crowding the three a_1 stretching vibrations in the narrow region 730–1110 cm^{-1} is certainly untenable, the lowest symmetric stretch with pulsation character being expected to lie below 400 cm^{-1} in $CF_3BF_3^-$ and similar systems. In addition a theoretically impossible $^{10/11}B$ shift of 50 cm^{-1} has been claimed for ν_{as} BF_3. Why the ν_1 frequency of C_2F_6 (this molecule is extremely useful for comparison) at 1420 cm^{-1} has been disregarded, although it has never been seriously in question,[8] is not understandable.[9] (iii) Our second strongest Raman line is a sharp, polarized feature near 1350 cm^{-1}, which has a $^{10/11}B$ shift of 16 cm^{-1} and coincides with an IR absorption. Surely this feature is an a_1 fundamental of $CF_3BF_3^-$. The 1100-cm^{-1} region of our spectra differs considerably, being much simpler and conclusive with respect to $^{10/11}B$ shifts if the KBr pellets are prepared carefully for the IR measurements. Due to different values and assignments for several fundamentals we obtain a force field which differs from that of ref 7 but which is consistent with well-defined force fields of related species.

In addition to our vibrational spectroscopic investigation, a single-crystal x-ray study of $K[CF_3BF_3]$ is reported. The latter yielded the first structural information on group 3 CF_3 derivatives. Besides offering a firm structural basis for the interpretation of the vibrational spectrum, the distances and angles derived give useful clues to the bonding of CF_3 groups to electropositive elements.

Experimental Section

Preparation. $K[CF_3BF_3]$ was prepared by the reaction of $(CH_3)_3SnCF_3$ with BF_3 and subsequent solvolysis with aqueous KF solution.[5] BF_3 was obtained by heating natural (80.4% ^{11}B) and ^{10}B enriched H_3BO_3 (92.4% ^{10}B; Oak Ridge National Laboratory) with an equivalent amount of CaF_2 and concentrated sulfuric acid in a Monel cylinder (Hoke) and was purified by a standard vacuum technique before use. Samples of $K[CF_3BF_3]$ were purified by repeated recrystallization from absolute EtOH; then larger single crystals were grown from aqueous solution.

Infrared and Raman Spectra. Infrared spectra of KBr (0.5–8 mg/100 mg) and polyethylene (1.5–3 mg/100 mg) pellets were recorded in the 4000–200 and 400–50-cm^{-1} regions with the instruments Beckman IR 12 and Polytec FIR 30, respectively. Accuracy (not corrected for vacuum) of sharp features is ±0.5 cm^{-1}, resolution